High critical current densities in Nb47%Ti multilayers with a planar copper flux pinning nanostructure

E. Kadyrov, A. Gurevich, and D. C. Larbalestier
Applied Superconductivity Center, University of Wisconsin, Madison, Wisconsin 53706

(Received 30 August 1995; accepted for publication 9 January 1996)

The critical current densities (J_c) of Nb47 wt% Ti–Cu multilayers were investigated for the Nb–Ti layer thickness ranging from $d_s=10$ to 100 nm and for fixed Cu thickness $d_n=10$ nm. J_c showed a strong enhancement with decreasing d_s, reaching new very high values in this system [0.91 MA/cm^2 (5 T) and 0.38 MA/cm^2 (7 T)] for $d_s=30$ nm, declining at smaller d_s. The nonmonotonic dependence of J_c on d_s arises from competition between the enhanced pinning force produced by the increased pin density at smaller d_s which is opposed by a proximity-effect-induced depression of T_c at smaller superconductor thickness. © *1996 American Institute of Physics.* [S0003-6951(96)03311-3]

Understanding the physical mechanisms which limit the current-carrying capacity of superconductors and raising J_c towards such limits are both of great importance. Nb–Ti superconductor with artificial pinning centers (APC)[1–4] can exhibit maximum J_c substantially higher than conventionally optimized Nb–Ti. However, the enhancement of flux pinning in APC composites is usually accompanied by a proximity effect reduction in the upper critical field B_{c2}, which limits their performance at high fields.[2] There are two important factors which affect the J_c, T_c, and B_{c2} of APC conductors. First, is the choice of the superconducting matrix and the pin material, and the second is their geometry, in particular, the size of the individual pins and the separation between them.[1] Since the final shape of the pinning centers in real APC conductors usually turns out to be quite irregular, it is difficult to quantify the microstructure of the optimum pinning network[4] which, in turn, makes it difficult to optimize selection of the best materials for APC production wires. Given these uncertainties, it is not surprising that the ultimate limit of J_c of APC wires is unclear. In order to clarify these issues we have made model multilayer structures in which both the pin geometry and pin composition can be changed in a controlled way.

In this letter we report on the J_c of dc magnetron sputtered Nb47%Ti–Cu multilayers with varying thicknesses of Nb–Ti (d_s) and a constant Cu thickness (d_n). Here, d_s was varied in the 10–100 nm range, while $d_n=10$ nm was kept fixed so as to match the fluxon core size, 2ξ(4.2 K). Very high values of $J_c=0.91$ MA/cm^2 at 5 T and 0.38 MA/cm^2 at 7 T were observed in the sample with $d_s=30$ nm and $d_n=10$ nm. We found that $J_c(d_s)$ is a nonmonotonic function of d_s, having a pronounced maximum at an optimum d_s. The maximum in $J_c(d_s)$ is interpreted as being due to a competition between the suppression of T_c and H_{c2} by the proximity effect and the enhancement of flux pinning by increasing pin fraction at smaller d_s.

The multilayers were fabricated by two-gun dc-magnetron sputtering onto (1102) 5 mm×10 mm sapphire substrates held at room temperature. The base pressure p of the sputtering system was 5×10^{-8} Torr and the deposition was done in Ar plasma at $p=2$ mTorr. The multilayer structure was obtained by programmable positioning of the substrate in front of the sputtering guns which had Nb 47 wt % Ti and Cu targets of 99.9% and 99.99% purity, respectively. Cu was deposited at 75 W power and Nb 47 wt % Ti with 250 W power applied to the target, resulting in deposition rates of 12.1 Å/s and 10.6 Å/s for Nb–Ti and Cu, respectively. The thickness of individual layers was determined from the deposition times and measured with an Alpha-Step 200 profilometer with an accuracy of about 5%. A 10 nm Cu layer was deposited onto the substrate before multilayer deposition and as a cap after it was complete.

A set of five samples was fabricated having $d_n=10$ nm and different d_s: 10, 30, 50, 70, and 100 nm. The total number of layers varied from 50 to 11 in order to maintain the total thickness at 1 μm. θ-2θ x-ray diffractometry scans showed two peaks at 38.78° (NbTi) and 43.07° (Cu) with intensities proportional to the volume fraction of the components. Low angle diffractometer scans had a distinct satellite peak structure reflecting a good multilayer periodicity. Modulation wavelengths calculated from low angle x-ray diffraction scans[5,6] were within 15% of the values expected from the deposition rates. Transmission electron microscopy on several samples confirmed periodic structure of the samples and previous size measurements. The samples were patterned photolithographically and etched with HF/HNO$_3$ to produce 50 μm wide by 3 mm long bridges. J_c, defined at 1 μV/cm, was measured by the four-probe method. The particular selection of the voltage criterion had little effect on observed J_c values since the samples exhibited very sharp resistive transition. The magnetic field $0<\mathbf{B}<12$ T was applied parallel to the layers and was always perpendicular to the transport current flowing along the layers. The field was aligned parallel to the layers by using a goniometer with an angular resolution of 0.015° by finding the maximum in the angular dependence of $J_c(\mathbf{B})$. Critical temperature T_c and the upper critical field B_{c2} were obtained by measuring the sample resistivity $R(T,H)$ and using the $R=0.01\%R_n$ criterion, where R_n is the normal state resistance.

The representative $J_c(B)$ curves shown in Fig. 1 exhibit a characteristic nonmonotonic $J_c(B)$ dependence with a low-field minimum in J_c, followed by a rise in J_c over a certain field range and then a decline of J_c as B is further increased. This effect increased with decreasing d_s, as previously

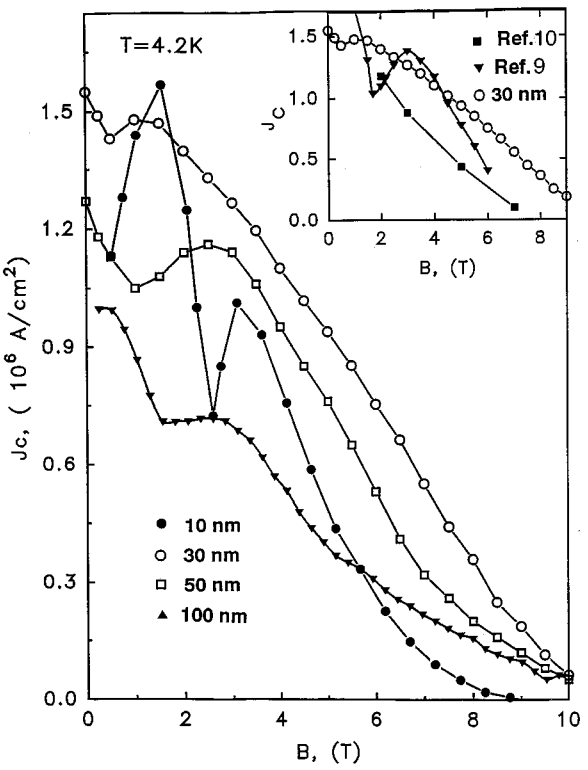

FIG. 1. Field dependencies of J_c at 4.2 K for multilayers with different superconductor thickness. The Cu layer thickness is 10 nm for all samples, and the Nb–Ti thickness is indicated on the graph. Inset shows the comparison of the 30 nm sample with the best Nb–Ti/Nb APC round wire of Ref. 10 and best Nb–Ti/Nb multilayer of Ref. 9 (data of Ref. 9 are taken at a 5° angle between the sample plane and applied field direction).

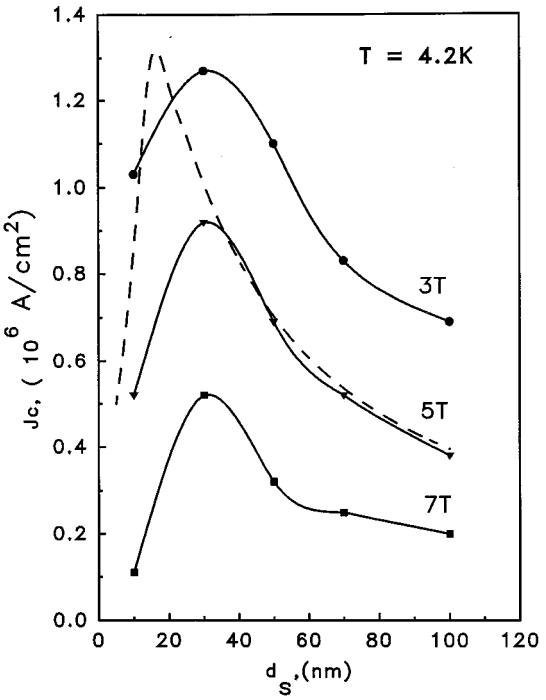

FIG. 2. $J_c(d_s)$ dependence at T=4.2 K for B=3, 5, and 7 T. The solid curves are guides to the eye. The dashed curve corresponds to Eq. (3). The coefficient of proportionality is the only fit parameter.

observed.[7,8] We found that B_{c2} first slightly increased for thinner d_s (10.7 T for 100 nm and 11 T for 30 nm), but then decreased to 8.7 T for $d_s=10$ nm. The 10 nm sample exhibited two sharp peaks in $J_c(B)$ at 1.7 and 3 T, which may be due to matching of the vortex lattice to the multilayer structure, whose period 20 nm is close to the spacing between neighboring vortex rows $(\sqrt{3}\phi_0/2B)^{1/2}\approx 22$ nm at 3.5 T. The inset to Fig. 1 compares the J_c of the 30 nm sample with the best published Nb–Ti/Nb multilayer[9] and APC wire[10] with randomly oriented Cu and Nb pins. The 30 nm sample displays J_c values which are more than twice as high as the best APC and conventionally optimized Nb–Ti materials in the crucial high field region $B>6$ T.[10] As seen from Fig. 1, both the APC wire of Ref. 2 and the Nb–Ti/Nb multilayer of Ref. 9 appear to have a more pronounced B_{c2} depression than our Nb–Ti/Cu multilayers with high purity (99.99%) Cu pins. A more detailed comparison of our data to the results of Refs. 2 and 9 is difficult since no information was available on the shape, final size, and purity of the Cu pinning centers in Ref. 2, and J_c data of Ref. 9 was taken at a 5° angle between the sample and magnetic field direction.

Figure 2 plots $J_c(d_s)$ for 3, 5, and 7 T, showing that J_c exhibits a peak around $d_s\approx 30$ nm. This may be attributed to the lower B_{c2} for $d_s=10$ nm due to the dependence of T_c on d_s shown in Fig. 3. Here, T_c declines from 8.3 to 6.6 K as d_s diminishes from 100 to 10 nm, and matrix/pin ratio goes from 10:1 to 1:1. The data imply a power-law dependence $T_c(d_s)$ typical for proximity-coupled systems:[11]

$$T_c=T_{c0}[1-(a/d_s)^{\alpha}], \tag{1}$$

where $T_{c0}=9.1$ K is the bulk critical temperature,[12] $a=1.85$ nm, and $\alpha=0.42$. The small values of $\alpha\sim 0.3\xi$ in Eq. (1) indicate strong proximity coupling and a weak T_c suppression, unlike, say, ferromagnetic multilayers for which $\alpha=2$.[11]

The thickness dependence of J_c in Fig. 2 can be due to the following physical mechanisms. Because of their good proximity coupling, the high purity Cu layers only weakly depress B_{c2}, thus behaving as planar high J_c Josephson contacts which provide very strong magnetic and core pinning of vortices which are closer than the effective interaction length $l\approx \xi J_d/J_p$.[13] Here, J_p is the density of tunneling supercurrent through the normal layers, $J_d\approx c\phi_0/16\pi^2\lambda^2\xi$ is the Nb–Ti depairing current density, ϕ_0 is the flux quantum, and c is the speed of light. In our best 30 nm multilayer, the half-thickness of Nb–Ti was only 3ξ, so the current density, $J(d_s/2)=c\phi_0/4\pi^2\lambda^2 d_s$ circulating at a distance $d_s/2$ from the core is comparable to J_d, which is $\approx 3\times 10^7$ A/cm^2 for Nb47 wt %Ti.[14] Since J_d is much higher than the J_p, which can be transmitted through even strongly proximity coupled Cu layers, we have $l\gg d_s$, so that any given vortex strongly interacts with many Cu layers. This implies that at distances $\sim d_s$ from the core, only a small fraction of the vortex screening currents can pass through the Cu pinning layers which thus effectively behave as insulating interfaces having very strong magnetic pinning comparable to that in a thin film of thickness $\sim d_s$.[13] In the case $2l>d_s$ the elementary pinning force f_p experienced by a vortex moving across the Nb–Ti layers can then be estimated from the well-known result for thin $(d_s\ll\lambda)$ films:[14–16]

$$f_p\sim\frac{1}{d_s}\left(\frac{\phi_0}{4\pi\lambda}\right)^2. \tag{2}$$

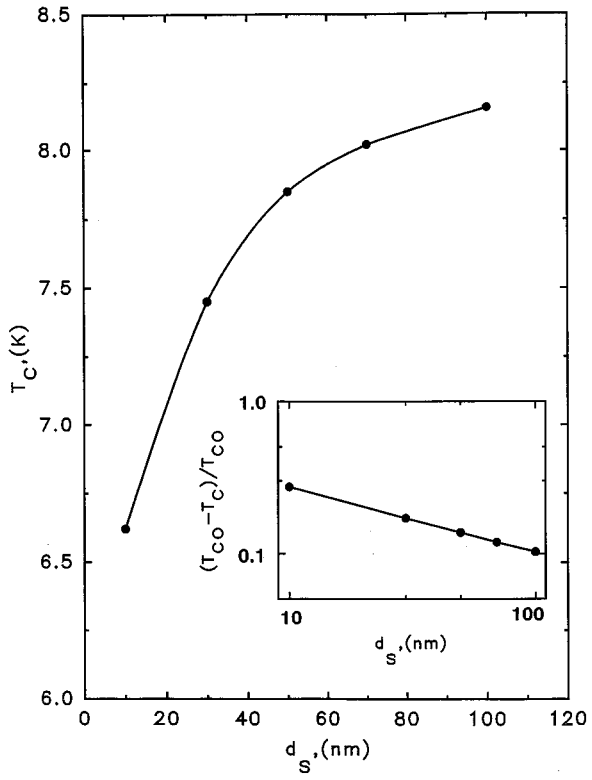

FIG. 3. Dependence of T_c upon the Nb–Ti thickness (Cu layer thickness is 10 nm for all samples).

Here, we neglect any possible anisotropy of λ due to multilayer structure because this should be weak in the case of the strong proximity coupling of these films. Since we are interested in the qualitative dependence of f_p upon d_s, the coefficient of proportionality in Eq. (2) is not discussed here. Assuming then $\lambda(T)=(1-T/T_c)^{-1/2}\lambda_0$, $J_c \sim c f_p/\phi_0$ and using Eq. (1), we arrive at

$$J_c \sim \frac{1}{d_s}\left(\frac{\phi_0}{4\pi\lambda_0}\right)^2\left(1-\frac{t}{1-(a/d_s)^\alpha}\right), \tag{3}$$

where $t=T/T_{c0}$. As seen from Eq. (3), the dependence $J_c(d_s)$ is nonmonotonic due to a competition between the increase of the pinning force with reducing d_s given by the first factor in Eq. (3) and the proximity effect T_c suppression described by the term in square brackets.. Therefore, to optimize flux pinning it is beneficial to decrease d_s by increasing the volume percent of pinning centers in the composite, an already well documented result.[4] However, T_c is depressed for small d_s, thus increasing λ and decreasing B_{c2}. The interplay between these two opposing trends produces the maximum in $J_c(d_s)$, the optimum thickness d_s^* being:

$$(a/d_s^*)^\alpha = 1+(\alpha-1)t/2-\sqrt{\alpha t+(\alpha-1)^2t^2/4}. \tag{4}$$

Substituting a and α from Eq. (1) into Eq. (4), we obtain for $T=4.2$ K ($t=0.46$) that $d_s^*=15.7$ nm, which is consistent with the observed optimum d_s^* being between 10 and 30 nm. As seen from Fig. 2, Eq. (3) gives also a good qualitative description of the observed behavior of $J_c(d_s)$, in particular, its $1/d_s$ dependence at larger d_s. In addition, Eq. (3) predicts that J_c of Nb–Ti/Cu multilayers could be improved even further by taking $d_s \approx 20$ nm. As T approaches T_c the optimum thickness $d_s^*(T)\approx[(1+\alpha)/(1-t)]^{1/\alpha}a$ increases, although remaining finite at T_c, since $T_c(d_s)<T_{c0}$, so $t=T_c(d_s)/T_{c0}$ is always smaller than 1.

This analysis leads us to believe that the very good high field performance of our Nb–Ti/Cu multilayers is due to two principal factors. First, the high initial purity of the Cu used as pins which have d_n much less than both the electron mean-free-path l_i and the proximity length $\xi_N=\hbar v_F/2\pi T$, minimizes the suppression of B_{c2}. Second, making the Nb–Ti thickness comparable to ξ, provides very strong magnetic pinning of vortices, since for $2l>d_s$ the Cu layers can result in flux pinning comparable to that obtained at a superconductor/vacuum interface. In this case J_c only weakly depends on the pin material properties and is rather determined by the geometry of flux pinning network.[13]

In conclusion, we have studied the critical current densities of the model Nb 47 wt %Ti–Cu multilayer system in order to experimentally probe the limits of J_c possible with optimized pinning arrays. We deliberately made the films several penetration depths thick so as to avoid thin film enhancements of J_c,[14] thus permitting better extrapolation to the case of real, many micron thick filament composites. Record high-field values of $J_c=0.91$ MA/cm^2 at 5 T and 0.38 MA/cm^2 at 7 T were observed in a 1 μm thick sample with 30 nm thick Nb–Ti layers. Our results demonstrate that there is a significant potential for further improvement of J_c of Nb–Ti composites by better selection of the pin material and geometry.

This work was supported by the U.S. Department of Energy, Division of High Energy Physics. The authors are grateful to W. Starch and A. Squitieri for valuable experimental assistance and to J. E. Nordman for use of some of his laboratory facilities.

[1] K. Matsumoto, Y. Tanaka, K. Yamafuji, K. Funaki, M. Iwakuma, and T. Matsushita, IEEE Trans. Appl. Supercond. **3**, 1362 (1993).
[2] L. Motowidlo and B. Zeitlin, Appl. Phys. Lett. **61**, 991 (1992).
[3] O. Miura, K. Matsumoto, Y. Tanaka, K. Yamafuji, N. Harada, M. Iwakuma, K. Funaki, and T. Matsushita, Cryogenics **32**, 315 (1992); O. Miura, I. Inoe, T. Suzuki, K. Matsumoto, Y. Tanaka, K. Funaki, M. Iwakuma, K. Yamafuji, and T. Matsushita, *ibid.* **35**, 169 (1995).
[4] P. Lee, P. Jablonski, and D. Larbalestier, IEEE Trans. Appl. Supercond. **5**, 1701 (1995).
[5] B. Y. Jin, Y. H. Shen, H. Q. Yang, H. K. Wong, J. E. Hillard, J. B. Ketterson, and I. K. Schuller, J. Appl. Phys. **57**, 2543 (1985).
[6] D. de Fontaine, in *Local Atomic Arrangements Studied by X-Ray Diffraction*, edited by J. B. Cohen and J. E. Hilliard (Gordon and Breach, New York, 1974), p. 51.
[7] H. Raffy, J. C. Renard, and E. Guyon, Solid State Commun. **11**, 1679 (1972).
[8] P. Korevaar, W. Maj, P. H. Kes, and J. Aarts, Phys. Rev. B **47**, 934 (1993).
[9] J. D. McCambridge, N. D. Rizzo, X. S. Ling, J. Q. Wang, D. E. Prober, L. R. Motowidlo, and B. A. Zeitlin, IEEE Trans. Appl. Supercond. **5**, 1697 (1994).
[10] K. Matsumoto, H. Takewaki, Y. Tanaka, O. Miura, K. Yamafuji, K. Funaki, M. Iwakuma, and T. Matsushita, Appl. Phys. Lett. **64**, 115 (1994).
[11] B. Y. Jin and J. B. Ketterson, Adv. Phys. **38**, 292 (1989).
[12] I. Banerjee and I. K. Schuller, J. Low Temp. Phys. **54**, 501 (1984).
[13] A. Gurevich and L. D. Cooley, Phys. Rev. B **50**, 13563 (1994).
[14] G. Stejic, A. Gurevich, E. Kadyrov, D. Christen, R. Joynt, and D. C. Larbalestier, Phys. Rev. B **49**, 1274 (1994).
[15] V. V. Schmidt, Sov. Phys. JETP **30**, 1137 (1970).
[16] Y. Mawatari and K. Yamafuji, Physica C **228**, 336 (1994).